Amino Acids (2015) 47:511–523
DOI 10.1007/s00726-014-1882-0

ORIGINAL ARTICLE

Enzymatic and non-enzymatic mechanisms of dimesna metabolism

Murray J. Cutler · Thomas J. Velenosi · Ankur Bodalia · Andrew A. House · Bradley L. Urquhart · David J. Freeman

Received: 8 April 2014 / Accepted: 22 November 2014 / Published online: 10 December 2014

Abstract The chemical reduction of the disulfide homodimer dimesna to its constituent mesna moieties is essential for its mitigation of nephrotoxicity associated with cisplatin and ifosfamide anticancer therapies and enhancement of dialytic clearance of the cardiovascular risk factor homocysteine. The objective of this study was to investigate potential enzymatic and non-enzymatic mechanisms of intracellular dimesna reduction. Similar to endogenous intracellular disulfides, dimesna undergoes thiol–disulfide exchange with thiolate anion-forming sulfhydryl groups via the two-step S_N2 reaction. Determination of equilibrium constants of dimesna reduction when mixed with cysteine or glutathione provided a mechanistic explanation for dramatic cysteine and homocysteine depletion, but sparing of the endogenous antioxidant glutathione, previously observed during mesna therapy. Dimesna was reduced by recombinant enzymes of the thioredoxin system; however, oxidation of NADPH by the glutaredoxin system was only observed in the presence of combined dimesna and reduced glutathione, suggesting formation of oxidized glutathione following an initial non-enzymatic reduction of dimesna. Production of mesna by enzymatic and non-enzymatic mechanisms in HeLa cell lysate following dimesna incubation was demonstrated by a loss in mesna production following protein denaturation and prediction of residual non-enzymatic mesna production by mathematical modeling of thiol–disulfide exchange reactions. Reaction modeling also revealed that mixed disulfides make up a significant proportion of intracellular thiols, supporting their role in providing additional nephroprotection, independent of direct platinum conjugation.

Keywords Mesna · Dimesna · Glutathione · Cysteine · Thiol exchange

Abbreviations

APN	Aminopeptidase N
DTNB	5,5′-Dithio-bis-2-nitrobenzoic acid
$E^{\circ\prime}_{MSSM/MSH}$	Half-cell potential of the dimesna/mesna redox system
EDTA	Ethylenediaminetetraacetic acid
ESRD	End-stage renal disease
CCBL	Cysteine-S-conjugate-β-lyase
Cys	Cysteine
Cys^{34}	Cysteine-34
CySSyC	Cystine
F	Faraday constant
FBS	Fetal bovine serum
GGT	Γ-Glutamyltranspeptidase
GR	Glutathione reductase

M. J. Cutler (✉)
School of Pharmacy, University of Waterloo, 200 University Ave W., Waterloo, ON, Canada
e-mail: murray.cutler.jr@gmail.com

T. J. Velenosi · B. L. Urquhart · D. J. Freeman
Department of Physiology and Pharmacology, Western University, London, ON, Canada

A. Bodalia
Department of Physiology, University of Toronto, Toronto, ON, Canada

A. A. House
Division of Nephrology, Department of Medicine, University Hospital, London, ON, Canada

B. L. Urquhart · D. J. Freeman
Division of Clinical Pharmacology, Department of Medicine, University Hospital, London, ON, Canada

B. L. Urquhart · D. J. Freeman
Lawson Health Research Institute, London, ON, Canada

GRX1	Human glutaredoxin
GS-mesna	Mesna-glutathione disulfide
GSH	Glutathione
GSSG	Glutathione disulfide
HPLC-FD	High-performance liquid chromatography with fluorescence detection
$k1–4$	Micro-rate constants
K_{eq}	Equilibrium constant
k_{obs}	Pseudo-first-order rate constants
M	Mesna moiety
MBB	Monobromobimane
MM	Dimesna
MM_0	Dimesna, starting concentration
NADPH	Nicotinamide adenine dinucleotide phosphate
pK_a	Acid dissociation constant
$\hat{R}$	Gas constant
R	Thiol moiety
RM	Oxidized thiol and mesna species
RR	Oxidized thiol species
$RSSM$	Mixed disulfide intermediate
T	Absolute temperature
TNB	3-Thio-6-nitrobenzoate
Trxr1	Rat thioredoxin reductase 1
TRX1	Human thioredoxin

Introduction

The metabolism of the chemoprotectant dimesna to its constituent mesna moieties is an essential step in the mitigation of ifosfamide-induced hemorrhagic cystitis and cisplatin-induced nephrotoxicity (Boven et al. 2002; Hensley et al. 2008; Kurowski and Wagner 1997). Interestingly, mesna does not attenuate the anticancer efficacy of concurrently administered ifosfamide. This has been attributed to the rapid metal-catalyzed oxidation of mesna to its disulfide dimer, dimesna, within plasma (Brock et al. 1981a, b, 1982). When given as a homocysteine-lowering therapy, however, the formation of dimesna following intravenous administration of mesna during dialysis may contribute to its lack of efficacy (Di Giuseppe et al. 2014).

In addition to homodimerization, mesna may form mixed disulfides with the low molecular weight thiols, cysteine (Cys), reduced glutathione (GSH), homocysteine, γ-glutamylcysteine, or cysteinylglycine. These mixed disulfides have been hypothesized to play an important role by providing additional nephroprotection through inhibition of the enzymes γ-glutamyltranspeptidase (GGT) and aminopeptidase N (APN); enzymes responsible for the conversion of cisplatin to reactive thiol-platinum species (Hausheer et al. 2010, 2011). Measuring the abundance of mixed disulfides will help estimate their contribution to the overall chemoprotection provided by mesna and dimesna therapies.

Within the plasma, a fraction of mesna also circulates covalently protein bound to cysteine-34 of albumin. Work by our laboratory and others has demonstrated that the formation of mesna-Cys^{34}-albumin following mesna and dimesna dosing can be exploited to increase the fraction of homocysteine available for clearance (Lauterburg et al. 1994; Stofer-Vogel et al. 1993; Pendyala et al. 2000, 2003; Urquhart et al. 2006, 2007a, b). Homocysteine is a non protein-forming amino acid intermediate of the methionine cycle and precursor of GSH biosynthesis (Finkelstein 1998; Selhub 1999). Elevated plasma total homocysteine [defined as the sum of all sulfhydryl, low molecular weight disulfide, and protein-bound homocysteine (Mudd et al. 2000)] is associated in a graded, independent manner with the development of cardiovascular disease and vascular access thrombosis amongst patients requiring chronic hemodialysis (Bostom and Lathrop 1997; Mallamaci et al. 2002; Moustapha et al. 1998; Robinson et al. 1996; Shemin et al. 1999). The ability of mesna to increase the dialyzable fraction of homocysteine by thiol–disulfide exchange at Cys^{34}-albumin in uremic plasma has motivated further expansion of the therapeutic applications of mesna to the treatment of hyperhomocysteinemia in end-stage renal disease (ESRD) (Urquhart et al. 2006, 2007a).

The redox equilibrium and metabolism of sulfhydryl mesna, and its disulfide dimesna, are key determinants of their therapeutic applications. The identification of renal uptake and efflux transporters of dimesna has demonstrated active secretion of mesna into the urine following intracellular reduction in proximal tubular cells (Cutler et al. 2012). Cellular redox homeostasis is maintained by members of the oxidoreductase family of enzymes, notably the thioredoxin and glutaredoxin systems, and the abundant redox buffers GSH and cyst(e)ine (Cys; CySSyC) (Holmgren 1989; Meister and Anderson 1983). These systems have previously been implicated in the metabolism of dimesna, yet the kinetics and contributions of enzymatic and non-enzymatic mechanisms remain to be elucidated (Shanmugarajah et al. 2009; Verschraagen et al. 2004).

The objective of this study was to investigate potential enzymatic and non-enzymatic mechanisms of dimesna metabolism. To determine the mechanisms underlying dimesna redox equilibrium in the presence of the two most abundant biological thiols, Cys and GSH, we sought to measure the kinetics of their respective reactions. Enzymatic activities of recombinant enzymes of the thioredoxin and glutaredoxin systems, mouse kidney and liver homogenates, and cell lysate were also measured. Finally, contributions of both enzymatic and non-enzymatic activities were highlighted by mathematical modeling of non-enzymatic thiol–disulfide exchange.

Materials and methods

Materials

Bovine insulin, 5,5′-dithio-bis-2-nitrobenzoic acid (DTNB), oxidized glutathione (GSSG), GSH, mesna, nicotinamide adenine dinucleotide phosphate (NADPH), ethylenediaminetetraacetic acid (EDTA), recombinant human glutaredoxin (thioltransferase-1, GRX1, UniProtKB ID # P35754, EC 1.8.4.2), glutathione reductase (GR, UniProtKB ID # P00390, EC 1.8.1.7), thioredoxin (TRX1, UniProtKB ID # P10599, EC 1.8.4.10), and purified rat thioredoxin reductase 1 (Trxr1, UniProtKB ID # O89049, EC 1.8.1.9) were purchased from Sigma–Aldrich Canada Ltd. (Oakville, Ontario). Monobromobimane (Thiolyte, MBB) was obtained from EMD Biosciences (Gibbstown, NJ). Dimesna was a kind gift from Dr. Gideon Koren (University of Toronto, Canada).

Enzymatic activity of purified glutaredoxin and thioredoxin systems

Activity of the glutaredoxin system comprised of 0.01 U glutaredoxin (14.15 nM), 0.01 U glutathione reductase (80.59 nM), and 1 mM NADPH was measured spectrophotometrically at 340 nm by the initial rate of oxidation of NADPH. Endogenous substrate GSSG (1 mM) was included in each assay as a positive control. Activity of the thioredoxin system comprised of 0.35 U thioredoxin (approximately 0.5 μM), 0.05 U thioredoxin reductase (11.75 nM), and 0.2 mM NADPH was measured spectrophotometrically at 340 nm by the initial rate of oxidation of NADPH. Insulin (0.016 mM) was included in each assay as a positive control. Inhibition of the reduction of 1 mM DTNB by thioredoxin reductase in the presence of 1 mM dimesna and 1 mM NADPH was examined by monitoring the production of 3-thio-6-nitrobenzoate (TNB) from DTNB at 412 nm as previously described (Arner et al. 1999).

Dimesna reduction by human kidney cell line and enzymatic activity of tissue homogenates and cell lysate

Five female DBA/lacJ mice were anesthetised by isoflurane inhalation according to an Animal Use Protocol approved by the University Council on Animal Care. Liver and kidneys were removed and homogenized on ice with a motorized Tissue Tearor in PBS with 1 mM EDTA. Human cervical adenocarcinoma HeLa (ATCC # CCL-2) and HEK293 (ATCC # CRL-1573) human cell lines were cultured in DMEM (Lonza, Walkersville, Maryland) containing 10 % fetal bovine serum (FBS; Invitrogen, Carlsbad, CA), penicillin (50 U/mL) (Invitrogen), and streptomycin (50 μg/mL) (Invitrogen) at 37 °C in a humidified 5 % CO_2 atmosphere. Three passages of HeLa cells were grown to 80 % confluence, harvested by scraping, and lysed by repetitive freeze–thaw in PBS containing 1 mM EDTA. Total protein was measured by Pierce BCA protein kit (Pierce, Rockford, IL) and samples diluted in PBS containing 1 mM EDTA, aliquoted, and stored at −70 °C.

Monolayers of human embryonic kidney cells (HEK293) were incubated with 100 μM dimesna in Krebs–Henseleit bicarbonate buffer and collected by scraping. Cells were centrifuged at 400 g for 5 min and separated incubation buffer and cell pellets were stored at −70 °C. Thawed aliquots of cell pellets and incubation buffer were mixed with 25 μL of 12.5 mM MBB (25 % acetonitrile, 3 mM EDTA) followed by 25 μL of 50 mM Tris buffer (pH = 9.0) and then sonicated for 5 min (to lyse cells) prior to incubation at 37 °C for 15 min. Reaction mixtures were additionally treated with 25 μL of 15 % perchloric acid and centrifuged at 9,000 g for 5 min to precipitate proteins. Supernatant pH was adjusted to 4.0 by addition of 20 μL of 0.5 M citrate: 2.5 M sodium hydroxide solution prior to analysis.

Enzymatic activities of 1 mg/mL tissue homogenates and cell lysate supplemented with 1 mM NADPH were measured spectrophotometrically at 340 nm by the initial rate of oxidation of NADPH with and without 1 mM dimesna and 1 mM GSSG, alone and in combination.

Spectrophotometric assay of enzymatic activity

Assays of enzymatic activity were carried out using a Thermo Multiskan Spectrum spectrophotometer (Thermo Electron, Waltham, MA). Enzymatic activities of experiments utilizing NADPH as a cofactor were monitored by a decrease in absorbance at 340 nm at 1 min intervals for 60 min. Enzymatic activities of experiments utilizing DTNB as a substrate were monitored by an increase in absorbance at 412 nm due to the production of TNB at 10 s intervals for 5 min. All reaction mixtures were dissolved in PBS (pH = 7.0) containing 1 mM EDTA and pipetted in triplicate into clear 96-well plates warmed to 37 °C on a Zipvac 96 evaporator heating block (Glas-Col, Terre Haute, IN) to a final reaction volume of 200 μL. NADPH was added immediately prior to spectrophotometric measurements at 37 °C. Negative controls containing all reagents except dimesna or endogenous substrates were included in each assay to control for background absorbance.

Reduction of dimesna by non-enzymatic thiol–disulfide exchange and cell lysates

To detect the presence of an enzymatic reduction of dimesna in cell lysates, untreated and denatured lysates

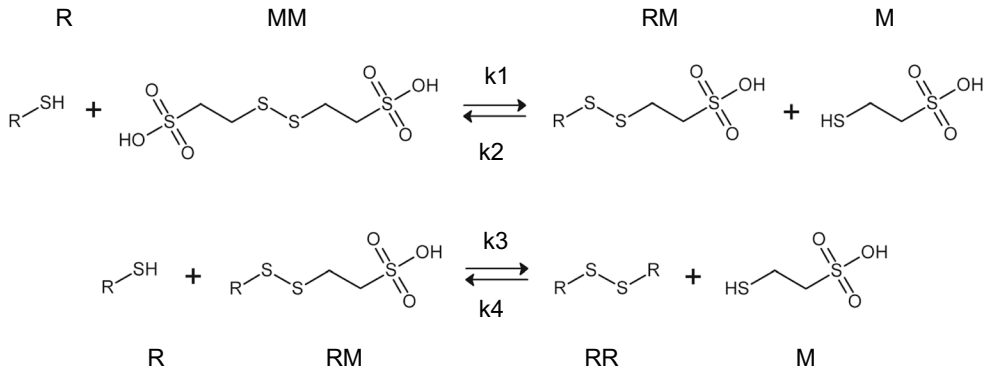

Fig. 1 Production of mesna by bimolecular nucleophilic substitution (S_N2) reactions whereby a nucleophilic thiol (e.g., Cys or GSH) first displaces a mesna moiety of dimesna yielding mesna and a mixed disulfide, followed by substitution of the mesna moiety of the mixed disulfide, producing a second molecule of mesna and a disulfide homodimer. Rate constants *k*1, *k*2, *k*3, *k*4 and species *R*, *MM*, *RM*, *RR*, and *M* denote parameters and variables, respectively, of Eqs. 1–6 describing equilibrium kinetics

were incubated with 1 mM dimesna and mesna production was measured following fluorescence derivatization. Redox enzymes were inactivated and removed by heating lysate at 95 °C for 5 min followed by centrifugation at 14,000 g for 10 min. Dimesna was added to a final concentration of 1 mM immediately prior to incubation of lysates in 1.7 mL microcentrifuge tubes at 37 °C. Non-enzymatic thiol–dimesna exchange was examined using final concentrations of dimesna, Cys, and GSH ranging from 10 to 3,000 µM diluted in PBS containing 1 mM EDTA and incubated in 1.7 mL microcentrifuge tubes at 37 °C. Aliquots of 50 µL were collected at 0, 5, 10, 15, 30, 60, and 90 min and transferred to a second microcentrifuge tube containing 25 µL of 12.5 mM MBB (25 % acetonitrile, 3 mM EDTA). Derivatization was initiated by addition of 25 µL of 50 mM Tris buffer (pH = 9.0) and incubation at 37 °C for 15 min. Cell lysates were additionally treated with 25 µL of 15 % perchloric acid and centrifuged at 9,000 g for 5 min to precipitate proteins. Supernatant pH was adjusted to 4.0 by addition of 20 µL of 0.5 M citrate: 2.5 M sodium hydroxide solution. Samples were diluted with 4 % acetonitrile: 96 % 25 mM ammonium formate buffer (pH = 3.75) as necessary prior to analysis.

Thiol analysis

Thiol analysis was conducted by high-performance liquid chromatography with fluorescence detection (HPLC-FD) with slight modification to methods previously described (Urquhart et al. 2006). Thiols derivatized with monobromobimane were injected onto a Zorbax SB-C18 column (150 × 3.2 mm, 5 µm particle) maintained at 40 °C in a Hewlett Packard 1090 LC (Agilent Technologies, Santa Clara, CA). Analytes were eluted with a gradient of 4 % acetonitrile: 96 % ammonium formate containing 0.75 mM dibutylamine (pH = 3.75) to 17 % acetonitrile: 83 % ammonium formate containing 0.75 mM dibutylamine (pH = 3.75) over 20 min at a flow rate of 0.5 mL min^{-1}. Retention times of derivatized Cys, GSH, and mesna were approximately 5.3, 8.3, and 12.5 min, respectively. Peaks were detected by a Waters 474 scanning fluorescence detector ($\lambda_{excitation}$ = 390 nm, $\lambda_{emission}$ = 480 nm; Waters, Milford, MA). The accuracy and precision of the assay were 1.3 and 2.0 %, respectively.

Determination of non-enzymatic thiol–disulfide exchange micro-rate constants

Similar to endogenous intracellular low molecular weight disulfide cystine (CySSyC), homocystine, and GSSG, we hypothesized that dimesna undergoes thiol–disulfide exchange with thiolate anion-forming sulfhydryl groups via an S_N2 reaction. This reaction is commonly presented as a two-step reaction, with each step describing the transfer of a single electron and subsequently the formation and consumption of the mixed disulfide intermediate (i.e., RSSM, Fig. 1) (Jocelyn 1972).

Given the equation:

$$MM_0 = M/2 + MM + RM/2 \tag{1}$$

where MM_0 is the starting dimesna molar concentration, and *M* and *MM* represent mesna and dimesna, respectively. Mixed mesna disulfide species are denoted as '*RM*'; consisting of a thiol moiety '*R*' and mesna moiety '*M*'. The reaction scheme can be quantified by a system of ordinary differential equations:

$$R' = k2 \times RM \times M - k1 \times R \times MM - k3 \times R \times RM + k4 \times RR \times M \tag{2}$$

$$MM' = k2 \times RM \times M - k1 \times R \times MM \tag{3}$$

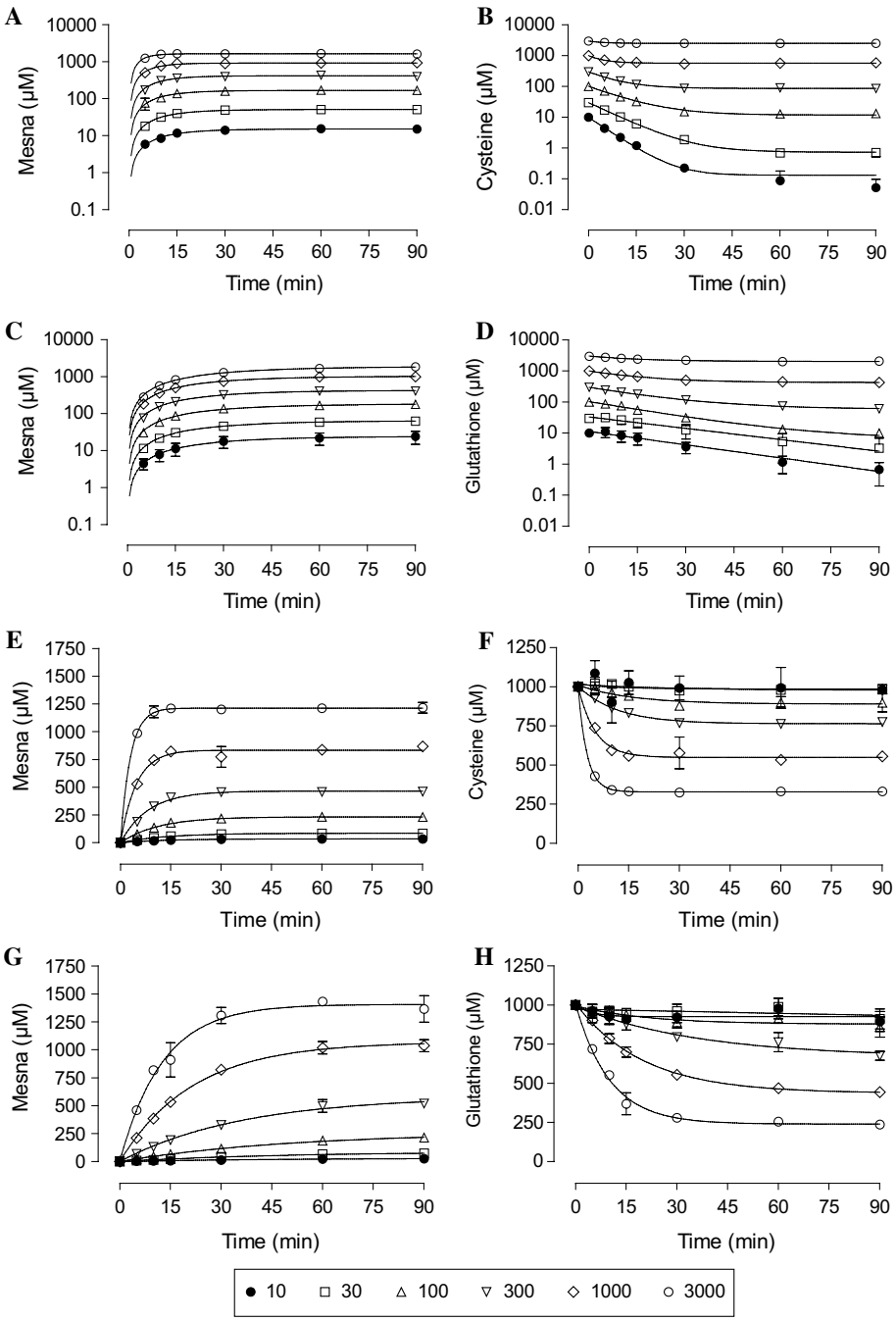

Fig. 2 Non-enzymatic reduction of 1 mM dimesna by different concentrations of Cys (**a**, **b**) and GSH (**c**, **d**) and non-enzymatic reduction of different concentrations of dimesna by 1 mM Cys (**e**, **f**) and 1 mM GSH (**g**, **h**). Fitted curves (*solid lines*) correspond to one-phase exponential association and one-phase exponential degradation of mesna production and thiol (Cys or GSH) loss. Starting thiol and dimesna concentrations are in micromolar. Mean ± SE of $N = 3$

$$RR' = k3 \times R \times RM - k4 \times RR \times M \quad (4)$$

$$RM' = k1 \times R \times MM - k2 \times RM \times M - k3 \times R \times RM + k4 \times RR \times M \quad (5)$$

$$M' = 2 \times (k1 \times R \times MM - k2 \times RM \times M + k3 \times R \times RM - k4 \times RR \times M) \quad (6)$$

where *RR* represents the oxidized species of the starting thiol. Second-order micro-rate constants $k1$, $k2$, $k3$, and $k4$ were estimated by simultaneous regression to both mesna and either Cys or GSH data presented in Fig. 2. Least-squares fitting was performed using Scientist software (Micromath Research, Salt Lake City, UT).

Modeling of non-enzymatic reduction of dimesna in cell lysate incubations

Dimesna, mesna, mesna-Cys, Cys, CySSyC, mesna-glutathione disulfide (GS-mesna), GSH, and GSSG concentration–time courses of untreated (total reactions) and denatured cell lysates (non-enzymatic reactions) were predicted

using basal Cys and GSH concentrations and supplemented dimesna concentration as initial values of differential Eqs. 2–6. Dimesna consumption and mesna production due to Cys and GSH exchange were summed. Mesna, Cys, and GSH concentration–time courses were regressed to observed values for calculation of coefficients of determination using Scientist software (Micromath Research).

Calculation of dimesna/mesna equilibrium constant

At equilibrium, the magnitude of flux between species, as determined by the product of the second-order rate constants and concentrations of species, is equal, thus the equilibrium constant for the dependent reactions can be derived as:

$$k1 \times R \times MM = k2 \times RM \times M \tag{7}$$

$$k3 \times R \times RM = k4 \times RR \times M \tag{8}$$

$$RM = (k4 \times RR \times M)/(k3 \times R)$$

Substituting Eq. 8 into Eq. 7 yields:

$$k1 \times R \times MM = (k2 \times k4 \times RR \times M^2)/(k3 \times R)$$
$$k1 \times k3 \times R^2 \times MM = k2 \times k4 \times RR \times M^2$$
$$(k1 \times k3)/(k2 \times k4) = (RR \times M^2)/(R^2 \times MM)$$

$$K_{eq} = (RR \times M^2)/(R^2 \times MM) = (k1 \times k3)/(k2 \times k4) \tag{9}$$

where K_{eq} represents the equilibrium constant.

Calculation of dimesna/mesna half-cell potential

Calculation of K_{eq} for dimesna in the presence of the standard biological reducing agent GSH facilitates indirect calculation of the half-cell potential of the dimesna/mesna redox system ($E^{\circ\prime}_{MSSM/MSH}$) by the Nernst equation:

$$E^{\circ\prime}_{MSSM/MSH} = E^{\circ\prime}_{GSSG/GSH} + (R \times T/n \times F) \times \ln\left(K_{eq}\right) \tag{10}$$

where $E^{\circ\prime}_{GSSG/GSH}$ is the half-cell potential of glutathione at pH 7.0 [−0.262 V (Millis et al. 1993)], $\hat{R}$ is the gas constant (8.314 J K^{-1} mol^{-1}), T is the absolute temperature of the reaction (310 K), n is the number of electrons transferred (2), and F is the Faraday constant (96,485 J V^{-1} mol^{-1}).

Data analysis and statistics

Observed pseudo-first-order rate constants ($k_{obs} = k \times MM$) were determined by fitting the first-order exponential association or decay functions to mesna or Cys/GSH concentration–time data, respectively. Significant differences between enzymatic activity of kidney and liver homogenates and cell lysates were determined using one-way ANOVA followed by Tukey's multiple comparison tests. Pairwise analysis of enzymatic data was performed using Student's t test. Pairwise analysis of fitted micro-rate constants was performed non-parametrically by Mann–Whitney U test. A $p < 0.05$ was considered a statistically significant difference. Curve fitting and statistics were conducted using Prism (GraphPad Software, Inc., San Diego, CA).

Results

Non-enzymatic reduction of dimesna

Fluorescence derivatization followed by HPLC-FD allowed for the simultaneous measurement of mesna, Cys, and GSH thiols following incubation in PBS containing 1 mM EDTA at 37 °C, pH = 7.0. The addition of EDTA facilitated the stabilization of thiols prior to the start of the experiment, but had no effect on the rate of thiol exchange in the presence of disulfide (data not shown) consistent with previously observations (Verschraagen et al. 2004).

Estimation of reaction order and macro-rate constants

Concentration–time courses of mesna production and corresponding thiol consumption following incubation of 1,000 μM dimesna with a range of Cys and GSH concentrations (10–3,000 μM) (Fig. 2a–d) and 1,000 μM Cys or GSH with a range of dimesna concentrations (10–3,000 μM; Fig. 2e–h) obeyed pseudo-first-order kinetics. The observed molar ratio of mesna production was approximately 2:1 for each mole of Cys or GSH consumed across all concentrations (mesna/Cys = 2.12 ± 0.27, mesna/GSH = 2.06 ± 0.14).

Plots of estimated velocities (0–10 or 0–15 min) were linear with slopes approximating unity at or below equimolar concentrations of reactants, indicating the rate of mesna production is first order for each of the reactants (Fig. 3a–d). The slope of the secondary plot of observed pseudo-first-order rate constants of mesna production yielded apparent second-order rate constants of 1.394×10^{-4} μM^{-1} min^{-1} and 0.275×10^{-4} μM^{-1} min^{-1} for reduction of dimesna by Cys and GSH, respectively (Fig. 3e, f).

Estimation of micro-rate constants

Measurement of both reactant (i.e., Cys and GSH) and product (i.e., mesna) sulfhydryls allowed for estimation of the micro-rate constants of Eqs. 2–6 describing the proposed thiol–disulfide reaction scheme (Fig. 1). Micro-rate

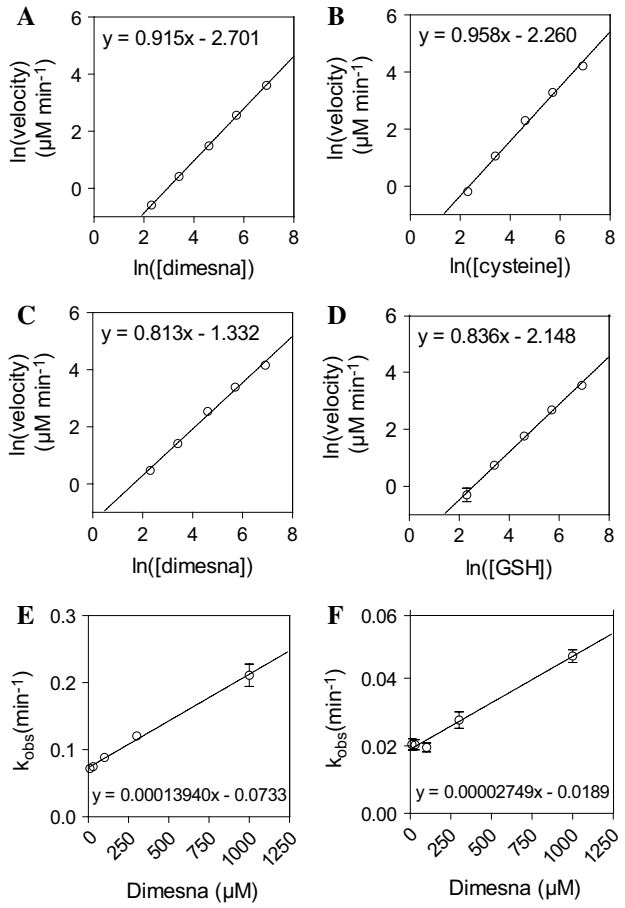

Fig. 3 Initial velocities of mesna production by dimesna with excess Cys (**a**), Cys with excess dimesna (**b**), dimesna with excess GSH (**c**), and GSH with excess dimesna (**d**). Slope of the lines indicate thiol exchange of dimesna is first order for each of the reactants. Observed first-order rate constants (k_{obs}) of mesna production in the presence of excess Cys (**e**) and GSH (**f**) versus starting dimesna concentrations. Slope of the line indicates second-order rate constant for the reduction of dimesna by Cys (**e**) and GSH (**f**). All concentrations are in micromolar. Mean ± SE of $N = 3$

constants that simultaneously fitted to mesna and Cys or GSH concentration–time courses are summarized in Table 1. Coefficients of determination were consistently high for predicted time courses of the reduction of dimesna by Cys (mesna $r^2 = 0.995 \pm 0.002$, Cys $r^2 = 0.983 \pm 0.011$) and GSH (mesna $r^2 = 0.969 \pm 0.022$, GSH $r^2 = 0.965 \pm 0.023$). Rate constants $k1$, $k2$, and $k3$ were significantly different between reactants Cys and GSH ($p < 0.05$, Table 1).

Calculation of dimesna redox equilibrium constants and half-cell potential of disulfide bond

Using rate constants listed in Table 1, the equilibrium constants of dimesna in the presence of Cys and GSH were calculated by Eq. 9 to be 0.200 and 1.697, respectively. Calculation of the half-cell potential of the dimesna disulfide bond in the presence of GSH (Eq. 10) resulted in a dimesna/mesna redox potential of −0.255 V.

Table 1 Estimated second-order micro-rate constants of S_N2 reaction scheme in Fig. 1, $N = 12$, p value calculated non-parametrically by Mann–Whitney U test

	Cys + dimesna 10^{-4} (μM min^{-1})		GSH + dimesna 10^{-4} (μM min^{-1})		p
	Mean	SE	Mean	SE	
$k1$	0.68	0.03	0.41	0.17	0.001
$k2$	1.65	0.28	3.22	2.57	0.004
$k3$	1.16	0.13	16.51	5.66	0.023
$k4$	2.40	0.61	1.23	0.23	0.301

Reduction of dimesna by thioredoxin and glutaredoxin systems

Enzymatic activities of purified enzymes and homogenates incubated at 37 °C in PBS containing 1 mM EDTA resulting in the oxidation of NADPH were monitored spectrophotometrically in the presence and absence of dimesna and known disulfide-containing substrates. An equimolar concentration of dimesna was unable to inhibit reduction of DTNB to 2-nitro-5-thiobenzoic acid (TNB) by thioredoxin reductase (1.64 ± 0.10 versus 1.67 ± 0.07 mAU TNB s^{-1}, $p = 0.733$). However, the thioredoxin system demonstrated a significant dimesna concentration-dependent increase in enzyme velocity (Fig. 4a), indicating that dimesna can be reduced directly by the thioredoxin system (Fig. 4b).

Incubation of glutathione reductase with its endogenous substrate, GSSG, resulted in rapid oxidation of NADPH that was not inhibitable by co-incubation with equimolar dimesna (17.97 ± 1.79 versus 18.49 ± 4.79 nmol NADPH min^{-1}, $p = 0.873$) suggesting dimesna does not bind to the catalytic site of glutathione reductase.

Upon addition of dimesna to the glutaredoxin system, no significant change in NADPH concentration was detected. However, co-incubation of dimesna with GSH facilitated a significant increase in enzymatic activity by the glutaredoxin system (3.48 ± 0.75 nmol NADPH min^{-1}) compared to either dimesna or GSH alone (−0.18 ± 0.57 and 0.30 ± 0.19 nmol NADPH min^{-1}, respectively, $p < 0.001$, Fig. 5a). A proposed mechanism of indirect dimesna reduction by the glutaredoxin system is summarized in Fig. 5b.

Enzymatic reduction of dimesna by human kidney cell line and tissue homogenates

Incubation of monolayers of HEK293 cells with dimesna resulted in linear export of mesna (Fig. 6a) confirming the capacity of intact renal cell systems to reduce dimesna

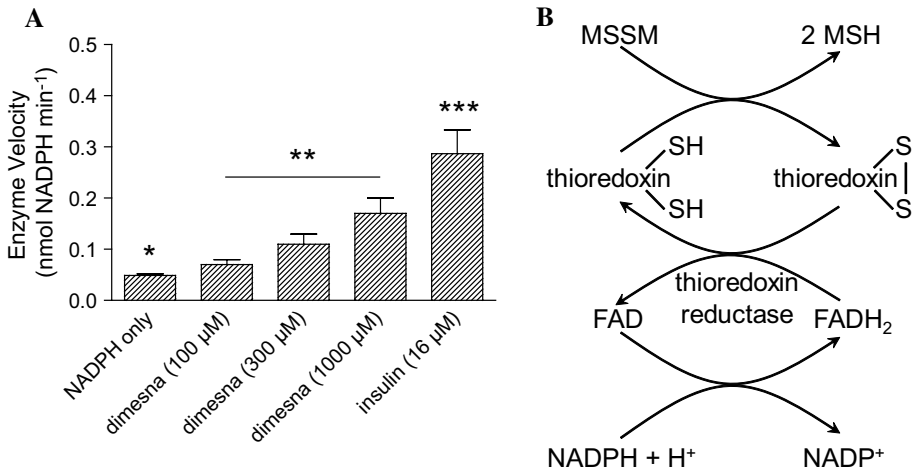

Fig. 4 **a** Reduction of dimesna by purified recombinant thioredoxin (500 nM) and thioredoxin reductase (11.75 nM) in PBS, 1 mM EDTA at 37 °C, pH = 7.0. Enzyme velocities were measured by analysis of NAD formed spectrophotometrically. Mean ± SE of $N = 3$. Differences between incubations determined by ANOVA *, **, ***$p < 0.01$. **b** Scheme of dimesna (MSSM) reduction by the thioredoxin system. The N-terminal active site Cys residue of thioredoxin $(SH)_2$ reduces protein disulfides by forming a transient mixed disulfide followed by fast thiol-disulfide exchange oxidizing a pair of reactive Cys at the active site producing thioredoxin$(S)_2$. Alternatively, reduced thioredoxin $(SH)_2$ may directly reduce dimesna to form two mesna moieties and thioredoxin$(S)_2$. Reduction of thioredoxin$(S)_2$ is facilitated by the flavoprotein thioredoxin reductase via electron transfer from NADPH

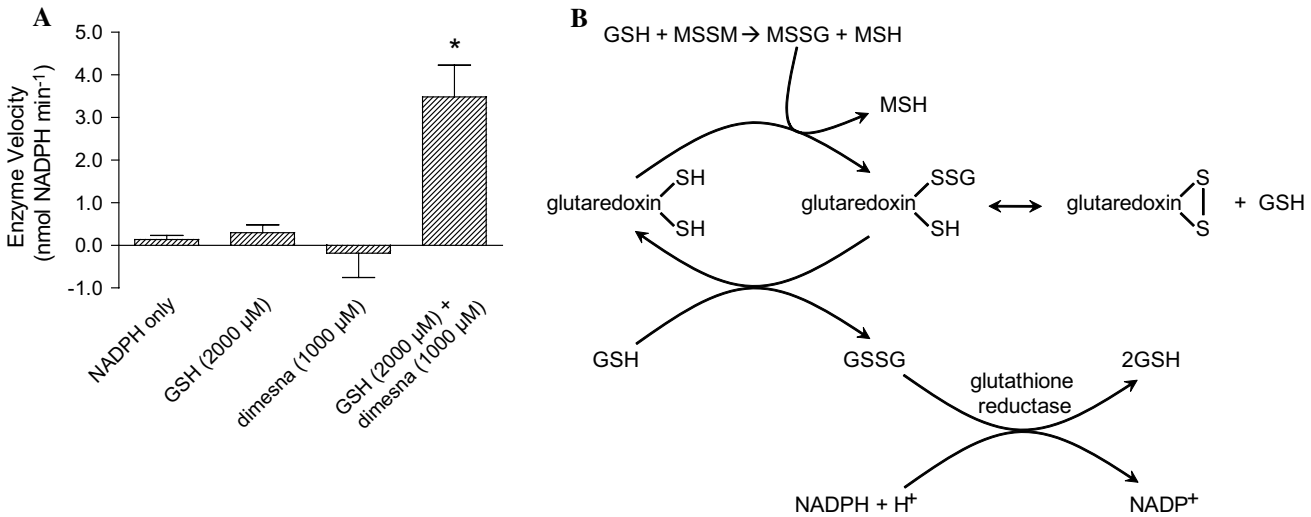

Fig. 5 **a** Reduction of dimesna by purified recombinant glutaredoxin (14.15 nM) and glutathione reductase (80.59 nM) in PBS, 1 mM EDTA at 37 °C, pH = 7.0. Enzyme velocities were measured spectrophotometrically. Mean ± SE of $N = 3$. Differences between incubations determined by ANOVA, *$p < 0.01$. **b** Scheme of dimesna (MSSM) reduction by the glutaredoxin system. Similar to thioredoxin, the N-terminal active site Cys residue of glutaredoxin $(SH)_2$ reduces protein disulfides by forming a transient mixed disulfide followed by fast thiol-disulfide exchange oxidizing a pair of reactive cysteines at the active site producing oxidized glutaredoxin$(S)_2$. Additionally, glutaredoxin $(SH)_2$ specifically reduces S-glutathionylated proteins and mixed disulfides, yielding a glutaredoxin-GSH conjugate. Dimesna (MSSM), although not a substrate of glutaredoxin, can first undergo non-enzymatic thiol exchange with GSH to produce the mixed mesna-glutathione disulfide (MSSG). MSSG can subsequently be reduced by glutaredoxin producing mesna and a glutaredoxin-GSH conjugate. The glutaredoxin-GSH conjugate can be reduced to glutaredoxin $(SH)_2$ by an additional molecule of GSH, forming oxidized glutathione (GSSG). Glutathione reductase recycles GSSG to two molecules of GSH via electron transfer from NADPH

(Cutler et al. 2012; Ormstad et al. 1983; Ormstad and Uehara 1982). Analysis of cell pellets revealed a rapid accumulation of intracellular mesna (Fig. 6b) suggesting the observation of dimesna reduction by intact cells is transporter dependent, necessitating the use of cell-free systems (i.e., tissue homogenates).

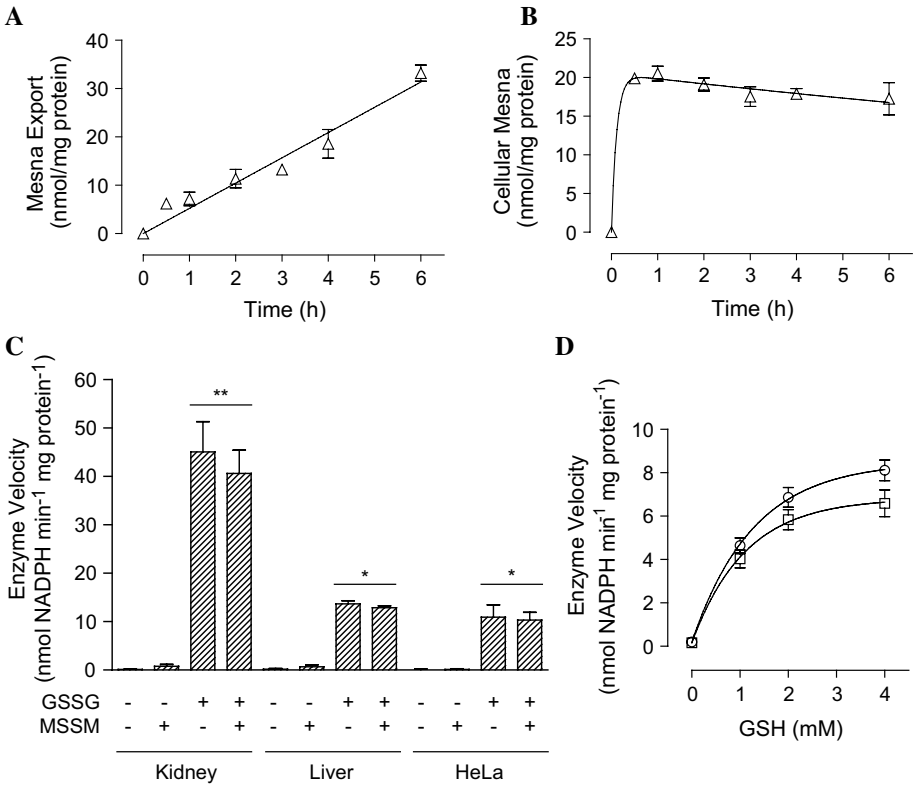

Fig. 6 **a** Export and **b** intracellular accumulation of mesna following incubation of HEK293 cell monolayers with 100 μM dimesna. Mean ± SE; $N = 3$. **c** Enzymatic activity of mouse kidney and liver homogenates, and HeLa cell lysates in the presence of 1 mM NADPH, 1 mM oxidized glutathione (GSSG) and/or 1 mM dimesna (MSSM). Mean ± SE of kidney and liver; $N = 5$, HeLa; $N = 3$. Differences between incubations determined by ANOVA, *, **$p < 0.01$. **d** Enzymatic activity of mouse kidney (*open circle*) and liver (*open square*) homogenates incubated with 1 mM NADPH, 1 mM dimesna, and increasing concentrations of reduced glutathione (GSH). Mean ± SE of $N = 5$

No enzymatic activity was observed with dimesna alone in mouse kidney and liver homogenates or HeLa cell lysate (Fig. 6c). The rate of GSSG reduction with and without dimesna was greater in kidney than liver and HeLa cell homogenates when normalized to protein concentration ($p < 0.001$, Fig. 6c). Enzymatic reduction of GSSG in all homogenates was unaltered by the presence of dimesna (Fig. 6c). Co-incubation of dimesna with increasing concentrations of GSH showed a saturable, concentration-dependent, increase in enzymatic activity that was equivalent between kidney and liver homogenates (kidney $k_{obs} = 0.79 \pm 0.14$ versus liver $k_{obs} = 0.90 \pm 0.22$ mM^{-1}, $p = 0.231$, Fig. 6d).

Contribution of enzymatic and non-enzymatic mechanisms of reduction of dimesna in HeLa cell lysates

Incubation of HeLa cell lysate with 1 mM dimesna yielded saturable mesna production (plateau = 87.7 ± 1.3 μM) and concurrent decrease of endogenous Cys and GSH (Fig. 7). Following denaturation, the concentration of mesna produced significantly decreased (plateau = 29.7 ± 1.2 μM, $p < 0.001$, Fig. 7a). Denaturation significantly decreased the basal GSH concentration (1.70 ± 0.04 μM versus 13.0 ± 0.08 μM, $p < 0.001$, Fig. 7c). No change in GSH concentration of denatured lysate was detected in the presence of dimesna ($p = 0.079$, Fig. 7c). Low molecular weight thiols cysteinylglycine, cysteinylglutamate, and homocysteine were not detected in HeLa cell lysates.

Application of Eqs. 1–6 describing a two-step thiol–disulfide exchange reaction (Fig. 1) enabled predictive modeling of the absolute contribution of non-enzymatic reduction of dimesna by cell lysate. Using fitted microrate constants (Table 1) and basal concentrations of endogenous thiols (i.e., Cys and GSH) the concentration–time courses of mesna, Cys, and GSH following incubation of HeLa lysates were predicted (Fig. 7; solid and dotted lines). Cysteine and GSH concentrations during incubation of HeLa lysate prior to denaturation were well predicted with *r*-squared values of 0.822 and 0.937, respectively. In contrast, prediction of mesna production due to non-enzymatic thiol–disulfide exchange alone accounted for only 58 % of total sulfhydryl mesna produced ($r^2 = 0.383$, Fig. 7a; solid line). The disparity between observed mesna (Fig. 7a; circles) and mesna predicted by non-enzymatic reduction alone (Fig. 7a; solid line) was likely due to the additional presence of enzymatically produced mesna. Following removal of enzyme activity by denaturation, remaining total sulfhydryl mesna production was more accurately predicted by Cys-mediated non-enzymatic reduction of dimesna with coefficients of determination of mesna and Cys concentration–time courses of 0.993 and 0.802, respectively, confirming the contribution of both enzymatic and non-enzymatic mechanisms of dimesna reduction within

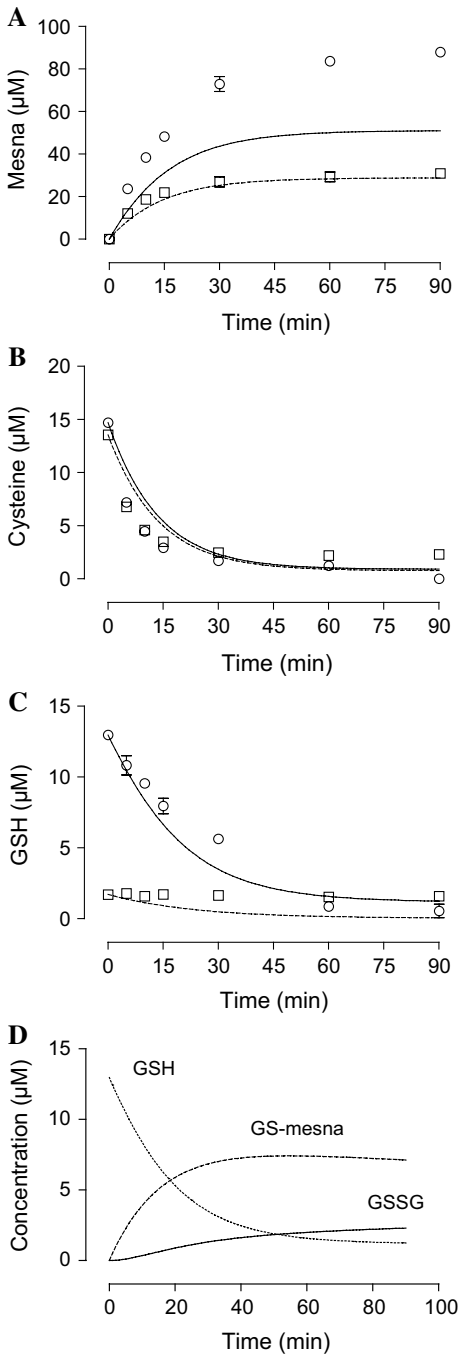

Fig. 7 Mesna (**a**), Cys (**b**), and GSH (**c**) concentrations following incubation of HeLa cell lysate (1 mg/mL in PBS, 1 mM EDTA) with 1 mM dimesna at 37 °C before (*open circle*) or after (*open square*) protein denaturation. Mean ± SE of $N = 3$. Predicted concentrations of thiol species due to non-enzymatic thiol exchange as described by Eqs. 1–6 using second-order rate constants listed in Table 1 and basal endogenous thiol concentrations of HeLa lysate before (*solid lines*) or after (*dashed lines*) denaturation are also plotted (**a**–**c**). Estimated GSH (*dotted*), GS-mesna (*dashed*), GSSG (*solid*) concentrations (**d**) given basal concentrations of GSH in un-denatured cell lysate

cell lysate. Modeling also facilitated estimation of disulfide GS-mesna, the precursor to mesna–cysteinylglutamate and mesna–cysteinylglycine disulfide species that may provide additional chemoprotection (Hausheer et al. 2010, 2011). Remarkably, GS-mesna concentrations were higher than GSSG and reached approximately 15 % of mesna levels, suggesting these newly identified chemoprotective species may reach clinically relevant concentrations (Fig. 7d).

Discussion

The reduction of dimesna to its two mesna thiol moieties is essential for conjugation of reactive metabolites of cisplatin and ifosfamide, attenuating otherwise dose-limiting toxicities and enabling their use in first-line chemotherapy (Boven et al. 2002; Hensley et al. 2008; Kurowski and Wagner 1997). To further expand the therapeutic application of mesna, in vitro experiments have shown that sulfhydryl mesna is capable of increasing the dialyzable fraction of homocysteine by thiol–disulfide exchange at albumin-Cys^{34} in uremic plasma (Urquhart et al. 2006). Thus, the redox equilibrium and metabolism of sulfhydryl mesna and its disulfide dimesna play an important role in their pharmacology.

As previously reported for other thiols (Gilbert 1995), the rate of thiol–disulfide exchange is dependent on the concentrations of both reactants (i.e., the 'thiol' and 'disulfide') hence the overall rate of dimesna consumption was expected to proceed via a second-order reaction. This is confirmed by the positive linear slopes of the plots of the observed pseudo-first-order rate constants with respect to dimesna in the presence of excess thiol. As anticipated from the steeper concentration–time courses of Cys compared to those of GSH, the second-order rate constant of Cys was approximately fivefold greater than that of GSH. This difference in reactivity is likely due to the lower acid dissociation constant of Cys [$pK_a = 8.2$–8.5 (Benesch and Benesch 1955)] than that of GSH [$pK_a = 8.7$ (Srinivasan et al. 1997)] ensuring greater ionization of the Cys thiol to a thiolate anion under physiological conditions.

Verschraagen et al. reported first-order rate constants for the net loss of dimesna when co-incubated with single concentrations of Cys or GSH (500 μM each). Consistent with our results, the authors reported the rate of loss of dimesna to be significantly higher when mixed with Cys than GSH (Verschraagen et al. 2004). Shanmugarajah et al. later expanded on the kinetics of non-enzymatic dimesna reduction by determining the forward and reverse second-order rate constants describing the transfer of the

first electron and formation of the mixed disulfide. The values of forward and reverse rate constants, although consistent with the single concentration of dimesna and thiol used (100 μM) may only represent apparent rate constants because of the omission of the transfer of the second electron and formation of the final oxidized thiol (i.e., CySSyC and GSSG) and may not accurately predict the quantity of mixed disulfide produced at equilibrium (Shanmugarajah et al. 2009).

To fully characterize the non-enzymatic mechanism of dimesna reduction by Cys and GSH, we sought to determine the second-order micro-rate constants of the differential equations describing the two reversible redox reactions. A number of observations regarding the tendency of thiol species to exchange with one another can be made from fitted rate constants. First, the rate of reaction between Cys and dimesna is likely the rate limiting step and may explain how an acceptable coefficient of determination could be obtained using only this first reaction (Shanmugarajah et al. 2009). The simple equilibrium constant of this first reaction ($k1/k2$) is approximately threefold greater for Cys than GSH, and within the two- to fivefold range of apparent first- and second-order rate constants reported here and previously (Shanmugarajah et al. 2009; Verschraagen et al. 2004). Also, the rate constants of the second reaction suggest different affinities of Cys and GSH species for mesna. Whereas formation of the mesna-Cys mixed disulfide is favored, and thus more stable than CySSyC, the reverse is true of GS-mesna, with GSSG existing as a more stable product. This pattern may be related to the relative differences in half-cell potentials. The redox potential of GSH ($E^{\circ\prime}_{\mathrm{RSSR/RSH}} = -0.262$) is slightly lower than that of Cys ($E^{\circ\prime}_{\mathrm{RSSR/RSH}} = -0.245$) at pH = 7.0, thus GSSG possesses a more stable disulfide bond than CySSyC (Jocelyn 1972; Millis et al. 1993).

To provide insight into the thermodynamic stability of dimesna compared to CySSyC and GSSG, the K_{eq} of the proposed reaction mechanism was derived. Calculation of K_{eq} of dimesna when mixed with Cys or GSH revealed K_{eq}s of 0.200 and 1.697, respectively. A $K_{eq} < 1$ implies the reverse reaction is more favored, suggesting dimesna is a more stable species than CySSyC. A $K_{eq} > 1$ of dimesna when mixed with GSH implies a tendency of the forward reaction to be favored, because it yields the more stable disulfide product GSSG (Millis et al. 1993). These observations are consistent with the existence of mesna moieties predominately as dimesna in patient plasma, despite circulating total Cys concentrations of approximately 300 μM, the majority of which exists in an oxidized form. In contrast, only approximately 3 μM of GSH is present in plasma to facilitate reduction of dimesna by a more favorable reaction (Pendyala et al. 2000; Masuda et al. 2011; Verschraagen et al. 2003).

For comparison to previously established half-cell potentials of other endogenous and common therapeutic thiols, the half-cell potential of the disulfide bond of dimesna was determined indirectly using the equilibrium constant of dimesna in the presence of GSH and its established half-cell potential. The half-cell potential of mesna (−0.255 V) is similar to the redox potentials of therapeutic and endogenous thiols captopril (−0.287 V), cysteamine (−0.260 V), Cys (−0.245 V), GSH (−0.262 V), homocysteine (-0.256 V), and penicillamine (−0.243 V) and much like the redox potentials of these thiols, favors oxidation ($E^{\circ\prime}_{\mathrm{RSSR/RSH}} < 0$) (Jocelyn 1972; Millis et al. 1993). Thus, our findings provide a mechanistic explanation for the greater reduction of cystine and homocystine by mesna than for GSSG in vitro and clinical observations of dramatic Cys and homocysteine depletion with only a modest decline in GSH during mesna therapy (Pendyala et al. 2000; Lauterburg et al. 1994; Stofer-Vogel et al. 1993; Smith et al. 2003). The redox potential of dimesna/mesna further supports the development of mesna as a therapeutic thiol exchange agent in ESRD without depletion of the protective endogenous antioxidant GSH.

Enzymatic reduction of dimesna has been proposed to proceed via the thioredoxin system consisting of the 12 kDa *E. coli* protein thioredoxin (*trxA*; Trx1, UniProtKB ID # P0AA25) and 55 kDa bovine thioredoxin reductase (*TXNRD1*; TR1, UniProtKB ID # O62768, EC 1.8.1.9.) (Verschraagen et al. 2004). In the present study, we demonstrate a concentration-dependent increase in enzymatic activity of a thioredoxin system consisting of recombinant human thioredoxin and purified rat thioredoxin reductase in the presence of clinically relevant dimesna concentrations. Given that dimesna was unable to lower the rate of reduction of DTNB by thioredoxin reductase, dimesna is most likely reduced directly by thioredoxin.

Incubation of dimesna with 12 kDa glutaredoxin from rat liver (Grx1, UniProtKB ID # Q9ESH6, EC 1.8.4.2; formerly thiol transferase) and 53 kDa yeast glutathione reductase (Gr, UniProtKB ID # P41921, EC 1.8.1.7, formerly EC 1.6.4.2) increased the sulfhydryl concentration of the mixture at a rate similar to dialyzed cytosolic fractions of kidney homogenate (Ormstad et al. 1983). Reduction of dimesna by purified enzymes of the glutaredoxin system consisting of the 10 kDa *E. coli* protein glutaredoxin (Grx1, UniProtKB ID # P68688, EC 1.8.4.2) and yeast glutathione reductase when supplemented with GSH has also been reported using spectrophotometric measurement of NADPH oxidation. Consistent with the results of Verschraagen et al. using non-mammalian enzymes (Verschraagen et al. 2004), enzymatic activity of the human cytosolic glutaredoxin system was only observed following co-incubation of GSH with dimesna. This was corroborated by the inability of dimesna to inhibit reduction

of equimolar GSSG by glutathione reductase. The catalytic site of glutathione reductase is believed to be highly specific to the γ-glutamylcysteine residues of GSH (Meister and Anderson 1983), thus, the formation of glutathionylated mesna moieties (i.e., mixed disulfides) by chemical thiol–disulfide exchange of GSH with dimesna facilitates enzymatic activity.

Similar to findings from the purified glutaredoxin system, supplementing kidney and liver homogenates with GSH dramatically increased the enzymatic activity. The equivalency between kidney and liver homogenates, despite the greater reductive capacity of the kidney, suggests that formation of the glutathione–mesna-mixed disulfide represents the rate limiting step in GSH-mediated enzymatic reduction of dimesna. Our results suggest that GSH-dependent reduction of dimesna by kidney and liver derives from a combination of non-enzymatic GSH-dimesna exchange and glutaredoxin-catalyzed reduction of GS-mesna disulfides (Goren et al. 1998; Ormstad et al. 1983; Ormstad and Uehara 1982).

To elucidate the contributions of enzymatic and non-enzymatic mechanisms of dimesna reduction in HeLa cells, the concentration–time courses of thiols species were predicted in silico by our model of thiol–dimesna exchange using parameters from in vitro experiments. Application of the model using basal Cys and GSH concentrations resulted in good fits to observed Cys and GSH data, for both untreated and denatured lysates. Interestingly, predicted mesna production due to non-enzymatic thiol exchange alone could only account for just over half of the mesna found in untreated lysate, suggesting the existence of enzymatic mechanism(s) of dimesna reduction. Upon removal of cellular enzymes by denaturation, the residual mesna production was almost entirely accounted for by non-enzymatic Cys–dimesna exchange. Taken together, our results demonstrate for the first time that enzymatic reduction significantly contributes to the intracellular metabolism of dimesna.

In addition to prediction of product and reactant thiols, the use of micro-rate constants allows for calculation of concentrations of mixed disulfide reaction intermediates. The importance of the production of mesna-mixed disulfides containing a terminal γ-glutamate or glycinate moieties in the mitigation of cisplatin-induced nephrotoxicity has recently been proposed (Hausheer et al. 2010, 2011). Toxication of cisplatin proceeds by S-glutathionylation and sequential cleavage of glutamate, glycine, and Cys residues by GGT, APN, and finally cysteine-S-conjugate-β-lyase (CCBL) to form reactive thiolate-platinum species (Townsend et al. 2003; Hanigan et al. 1994, 1996, 2001). Mesna was previously believed to be the sole active metabolite of dimesna; able to directly conjugate to cisplatin, thereby preventing its metabolic activation. Hausheer et al. has since demonstrated that mesna-mixed disulfides such as mesna-cysteinyl-glutamate and mesna-cysteinyl-glycine can inhibit GGT and APN activities, respectively (Hausheer et al. 2010, 2011). Our finding that GS-mesna-mixed disulfide is formed by non-enzymatic GSH-dimesna exchange at concentrations approximately 15 % of intracellular mesna suggests that inhibition of the toxication pathway of cisplatin by mixed disulfides may represent an additional clinically relevant mechanism of chemoprotection. Greater chemoprotection may be gained through the synthesis of new mixed disulfides of mesna with cysteine-containing dipeptide moieties to inhibit toxication of platinum while maintaining a redox state that spares endogenous GSH loss.

Acknowledgments The authors are grateful to Dr. Jack Bend for his expert advice in preparation of this manuscript, Dr. Richard Kim for use of the Kim Lab spectrophotometer and Sara LeMay for her skilled animal work.

Conflict of interest A. A. House, B. L. Urquhart, and D. J. Freeman have applied for a patent for the use of mesna to lower homocysteine in patients with ESRD.

References

Arner ES, Zhong L, Holmgren A (1999) Preparation and assay of mammalian thioredoxin and thioredoxin reductase. Methods Enzymol 300:226–239

Benesch RE, Benesch R (1955) The acid stength of the –SH group in cysteine and related compounds. J Am Chem Soc 77:5877–5881

Bostom AG, Lathrop L (1997) Hyperhomocysteinemia in end-stage renal disease: prevalence, etiology, and potential relationship to arteriosclerotic outcomes. Kidney Int 52(1):10–20

Boven E, Verschraagen M, Hulscher TM, Erkelens CA, Hausheer FH, Pinedo HM, van der Vijgh WJ (2002) BNP7787, a novel protector against platinum-related toxicities, does not affect the efficacy of cisplatin or carboplatin in human tumour xenografts. Eur J Cancer 38(8):1148–1156

Brock N, Pohl J, Stekar J (1981a) Detoxification of urotoxic oxazaphosphorines by sulfhydryl compounds. J Cancer Res Clin Oncol 100(3):311–320

Brock N, Pohl J, Stekar J (1981b) Studies on the urotoxicity of oxazaphosphorine cytostatics and its prevention. 2. Comparative study on the uroprotective efficacy of thiols and other sulfur compounds. Eur J Cancer Clin Oncol 17(11):1155–1163

Brock N, Pohl J, Stekar J, Scheef W (1982) Studies on the urotoxicity of oxazaphosphorine cytostatics and its prevention–III. Profile of action of sodium 2-mercaptoethane sulfonate (mesna). Eur J Cancer Clin Oncol 18(12):1377–1387

Cutler MJ, Urquhart BL, Velenosi TJ, Meyer Zu, Schwabedissen HE, Dresser GK, Leake BF, Tirona RG, Kim RB, Freeman DJ (2012) In vitro and in vivo assessment of renal drug transporters in the disposition of mesna and dimesna. J Clin Pharmacol 52(4):530–542

Di Giuseppe D, Priora R, Coppo L, Ulivelli M, Bartalini S, Summa D, Margaritis A, Frosali S, Di Simplicio P (2014) The control of hyperhomocysteinemia through thiol exchange mechanisms by mesna. Amino Acids 46(2):429–439

Finkelstein JD (1998) The metabolism of homocysteine: pathways and regulation. Eur J Pediatr 157(Suppl 2):S40–S44

Gilbert HF (1995) Thiol/disulfide exchange equilibria and disulfide bond stability. Methods Enzymol 251:8–28

Goren MP, Hsu LC, Li JT (1998) Reduction of dimesna to mesna by the isolated perfused rat liver. Cancer Res 58(19):4358–4362

Hanigan MH, Gallagher BC, Taylor PT Jr, Large MK (1994) Inhibition of gamma-glutamyl transpeptidase activity by acivicin in vivo protects the kidney from cisplatin-induced toxicity. Cancer Res 54(22):5925–5929

Hanigan MH, Gallagher BC, Taylor PT Jr (1996) Cisplatin nephrotoxicity: inhibition of gamma-glutamyl transpeptidase blocks the nephrotoxicity of cisplatin without reducing platinum concentrations in the kidney. Am J Obstet Gynecol 175(2):270–273

Hanigan MH, Lykissa ED, Townsend DM, Ou CN, Barrios R, Lieberman MW (2001) Gamma-glutamyl transpeptidase-deficient mice are resistant to the nephrotoxic effects of cisplatin. Am J Pathol 159(5):1889–1894

Hausheer FH, Shanmugarajah D, Leverett BD, Chen X, Huang Q, Kochat H, Petluru PN, Parker AR (2010) Mechanistic study of BNP7787-mediated cisplatin nephroprotection: modulation of gamma-glutamyl transpeptidase. Cancer Chemother Pharmacol 65(5):941–951

Hausheer FH, Parker AR, Petluru PN, Jair KW, Chen S, Huang Q, Chen X, Ayala PY, Shanmugarajah D, Kochat H (2011) Mechanistic study of BNP7787-mediated cisplatin nephroprotection: modulation of human aminopeptidase N. Cancer Chemother Pharmacol 67(2):381–391

Hensley ML, Hagerty KL, Kewalramani T, Green DM, Meropol NJ, Wasserman TH, Cohen GI, Emami B, Gradishar WJ, Mitchell RB, Thigpen JT, Trotti A, Trotti A III, von Hoff D, Schuchter LM (2008) American Society of Clinical Oncology 2008 clinical practice guideline update: use of chemotherapy and radiation therapy protectants. J Clin Oncol 27(1):127–145

Holmgren A (1989) Thioredoxin and glutaredoxin systems. J Biol Chem 264(24):13963–13966

Jocelyn PC (1972) Biochemistry of the SH group. Academic Press, New York

Kurowski V, Wagner T (1997) Urinary excretion of ifosfamide, 4-hydroxyifosfamide, 3- and 2-dechloroethylifosfamide, mesna, and dimesna in patients on fractionated intravenous ifosfamide and concomitant mesna therapy. Cancer Chemother Pharmacol 39(5):431–439

Lauterburg BH, Nguyen T, Hartmann B, Junker E, Kupfer A, Cerny T (1994) Depletion of total cysteine, glutathione, and homocysteine in plasma by ifosfamide/mesna therapy. Cancer Chemother Pharmacol 35(2):132–136

Mallamaci F, Zoccali C, Tripepi G, Fermo I, Benedetto FA, Cataliotti A, Bellanuova I, Malatino LS, Soldarini A (2002) Hyperhomocysteinemia predicts cardiovascular outcomes in hemodialysis patients. Kidney Int 61(2):609–614

Masuda N, Negoro S, Hausheer F, Nakagawa K, Matsui K, Kudoh S, Takeda K, Yamamoto N, Yoshimura N, Ohashi Y, Fukuoka M (2011) Phase I and pharmacologic study of BNP7787, a novel chemoprotector in patients with advanced non-small cell lung cancer. Cancer Chemother Pharmacol 67(3):533–542

Meister A, Anderson ME (1983) Glutathione. Annu Rev Biochem 52:711–760

Millis KK, Weaver KH, Rabenstein DL (1993) Oxidation/reduction potential of glutathione. J Org Chem 58:4144–4146

Moustapha A, Naso A, Nahlawi M, Gupta A, Arheart KL, Jacobsen DW, Robinson K, Dennis VW (1998) Prospective study of hyperhomocysteinemia as an adverse cardiovascular risk factor in end-stage renal disease. Circulation 97(2):138–141

Mudd SH, Finkelstein JD, Refsum H, Ueland PM, Malinow MR, Lentz SR, Jacobsen DW, Brattstrom L, Wilcken B, Wilcken DE, Blom HJ, Stabler SP, Allen RH, Selhub J, Rosenberg IH (2000) Homocysteine and its disulfide derivatives: a suggested consensus terminology. Arterioscler Thromb Vasc Biol 20(7):1704–1706

Ormstad K, Uehara N (1982) Renal transport and disposition of Na-2-mercaptoethane sulfonate disulfide (dimesna) in the rat. FEBS Lett 150(2):354–358

Ormstad K, Orrenius S, Lastbom T, Uehara N, Pohl J, Stekar J, Brock N (1983) Pharmacokinetics and metabolism of sodium 2-mercaptoethanesulfonate in the rat. Cancer Res 43(1):333–338

Pendyala L, Creaven PJ, Schwartz G, Meropol NJ, Bolanowska-Higdon W, Zdanowicz J, Murphy M, Perez R (2000) Intravenous ifosfamide/mesna is associated with depletion of plasma thiols without depletion of leukocyte glutathione. Clin Cancer Res 6(4):1314–1321

Pendyala L, Schwartz G, Smith P, Zdanowicz J, Murphy M, Hausheer F (2003) Modulation of plasma thiols and mixed disulfides by BNP7787 in patients receiving paclitaxel/cisplatin therapy. Cancer Chemother Pharmacol 51(5):376–384

Robinson K, Gupta A, Dennis V, Arheart K, Chaudhary D, Green R, Vigo P, Mayer EL, Selhub J, Kutner M, Jacobsen DW (1996) Hyperhomocysteinemia confers an independent increased risk of atherosclerosis in end-stage renal disease and is closely linked to plasma folate and pyridoxine concentrations. Circulation 94(11):2743–2748

Selhub J (1999) Homocysteine metabolism. Annu Rev Nutr 19:217–246

Shanmugarajah D, Ding D, Huang Q, Chen X, Kochat H, Petluru PN, Ayala PY, Parker AR, Hausheer FH (2009) Analysis of BNP7787 thiol-disulfide exchange reactions in phosphate buffer and human plasma using microscale electrochemical high performance liquid chromatography. J Chromatogr B Analyt Technol Biomed Life Sci 877(10):857–866

Shemin D, Lapane KL, Bausserman L, Kanaan E, Kahn S, Dworkin L, Bostom AG (1999) Plasma total homocysteine and hemodialysis access thrombosis: a prospective study. J Am Soc Nephrol 10(5):1095–1099

Smith PF, Booker BM, Creaven P, Perez R, Pendyala L (2003) Pharmacokinetics and pharmacodynamics of mesna-mediated plasma cysteine depletion. J Clin Pharmacol 43(12):1324–1328

Srinivasan U, Mieyal PA, Mieyal JJ (1997) pH profiles indicative of rate-limiting nucleophilic displacement in thioltransferase catalysis. Biochemistry 36(11):3199–3206

Stofer-Vogel B, Cerny T, Kupfer A, Junker E, Lauterburg BH (1993) Depletion of circulating cyst(e)ine by oral and intravenous mesna. Br J Cancer 68(3):590–593

Townsend DM, Deng M, Zhang L, Lapus MG, Hanigan MH (2003) Metabolism of cisplatin to a nephrotoxin in proximal tubule cells. J Am Soc Nephrol 14(1):1–10

Urquhart BL, House AA, Cutler MJ, Spence JD, Freeman DJ (2006) Thiol exchange: an in vitro assay that predicts the efficacy of novel homocysteine lowering therapies. J Pharm Sci 95(8):1742–1750

Urquhart BL, Freeman DJ, Spence JD, House AA (2007a) The effect of mesna on plasma total homocysteine concentration in hemodialysis patients. Am J Kidney Dis 49(1):109–117

Urquhart BL, Freeman DJ, Spence JD, House AA (2007b) Mesna as a nonvitamin intervention to lower plasma total homocysteine concentration: implications for assessment of the homocysteine theory of atherosclerosis. J Clin Pharmacol 47(8):991–997

Verschraagen M, Boven E, Ruijter R, van der Born K, Berkhof J, Hausheer FH, van der Vijgh WJ (2003) Pharmacokinetics and preliminary clinical data of the novel chemoprotectant BNP7787 and cisplatin and their metabolites. Clin Pharmacol Ther 74(2):157–169

Verschraagen M, Boven E, Torun E, Hausheer FH, Bast A, van der Vijgh WJ (2004) Possible (enzymatic) routes and biological sites for metabolic reduction of BNP7787, a new protector against cisplatin-induced side-effects. Biochem Pharmacol 68(3):493–502